



## City Research Online

### City, University of London Institutional Repository

---

**Citation:** Gonschior, C. P., Klein, K.-F., Sun, T. & Grattan, K. T. V. (2013). Generation of periodic surface structures on silica fibre surfaces using 405 nm CW diode lasers. *Journal of Non-Crystalline Solids*, 361(1), pp. 106-110. doi: 10.1016/j.jnoncrysol.2012.11.004

This is the unspecified version of the paper.

This version of the publication may differ from the final published version.

---

**Permanent repository link:** <https://openaccess.city.ac.uk/id/eprint/2053/>

**Link to published version:** <https://doi.org/10.1016/j.jnoncrysol.2012.11.004>

**Copyright:** City Research Online aims to make research outputs of City, University of London available to a wider audience. Copyright and Moral Rights remain with the author(s) and/or copyright holders. URLs from City Research Online may be freely distributed and linked to.

**Reuse:** Copies of full items can be used for personal research or study, educational, or not-for-profit purposes without prior permission or charge. Provided that the authors, title and full bibliographic details are credited, a hyperlink and/or URL is given for the original metadata page and the content is not changed in any way.

---

---

---

City Research Online:

<http://openaccess.city.ac.uk/>

[publications@city.ac.uk](mailto:publications@city.ac.uk)

---

# Generation of periodic surface structures on silica fibre surfaces using 405 nm CW diode lasers

C. P. Gonschior<sup>a,b</sup>, K.-F. Klein<sup>a</sup>, T. Sun<sup>b</sup> and K. T. V. Grattan<sup>b</sup>

<sup>a</sup>Technische Hochschule Mittelhessen, Competence Centre “Optical Technologies and Systems”,  
Wilhelm-Leuschner-Str. 13, 61169 Friedberg, Germany,

e-mail: cornell.p.gonschior@iem.thm.de, phone: +49-6031-604 218, fax: +49-6031-604 2082

<sup>b</sup>City University London, Northampton Square, London EC1V 0HB, United Kingdom

## ABSTRACT

Periodic surface structures have been observed on the end surfaces of synthetic silica fibres when they are exposed to long-term irradiation with light from a 405 nm CW diode laser. The surface structures are generated when the laser power is at a level which is three magnitudes of order lower than that of the damage threshold. They exhibit multiple bends, break-ups and bifurcations, unlike interference patterns but rather like the effect caused by short-pulsed laser irradiation on wide band-gap insulators. The detailed investigation undertaken in this work has concluded that the key parameters that contribute to the generation of the surface structures are power density, surface roughness, polarisation direction and the presence of ultraviolet defect centres.

*PACS Keywords:* single-mode laser, single-mode fibre, surface damage, periodic surface structures, ultraviolet defect centres

## 1 INTRODUCTION

Most fibre-optic systems available for the UV region use multi-mode fibres (MMF). The fibre comprises a core of high-OH (> 800 ppm) pure synthetic silica and a fluorine-doped cladding. These systems typically use broadband light sources, e.g. deuterium lamps, or high-power lasers, e.g. excimer lasers (193 nm, 248 nm, 308 nm) or third and fourth harmonic of Nd:YAG lasers (355 nm, 266 nm). For deep-UV (170 – 280 nm) applications with these light sources, the existence and transformation of different UV defect centres have been studied in detail [1,2,3,4]. The most prominent defect centres in silica fibres are related to an oxygen vacancy [5]. They can be distinguished as the oxygen deficiency centre ODC(I) at 7.6 eV (163 nm), the  $E'_\gamma$  centre at 5.8 eV (214 nm), and the oxygen deficiency centre ODC(II) at 4.9-5.2 eV (240 – 255 nm). Other defects are oxygen excess related, such as the non-bridging oxygen hole centre (NBOHC) at 4.67 eV (266 nm), and the peroxy linkage (POL) at 3.76 eV (330 nm). Improvements in the manufacturing process have

lead to UV fibres with significantly lower solarisation, i.e. less generated defect centres during operation, in the deep-UV region [6,7].

When MMF are used for high-power excimer laser light delivery [8,9], the surface damage threshold of synthetic silica is the primary limit. Severe optical damage is observed at power densities above 1 GW/cm<sup>2</sup> for pulsed lasers [10]. The generation and transformation of defect centres during operation is a second limit. The absorption bands of E'<sub>γ</sub> centres and ODC(II) strongly influence the ArF and KrF wavelengths at 193 nm and 248 nm, respectively [11]. When the existence of two different kinds of oxygen deficiency centres was discovered, it was also found that an ODC(II) can be photobleached to an E'<sub>γ</sub> centre by excimer laser irradiation [12,13].

Recent applications of fibre-optic systems in the near-UV require smaller spot sizes or better beam qualities that are not achievable with MMF [14]. High-OH synthetic silica single-mode fibres (SMF) with mode-field diameters from 2 to 3 μm for delivery of UV light fulfil these requirements. They are commercially available for the near-UV region (300 – 400 nm) and can be combined with light from continuous-wave (CW) single-mode diode lasers (375 nm, 395 nm, 405 nm). These single-mode lasers (SML) are under constant development and achieve high output powers in the range of 100 to 300 mW. If this high-power laser light is focused to beam waist diameters of about 2.5 μm for coupling to a SMF, power densities in the range of 2 to 6 MW/cm<sup>2</sup> are reached.

An effect, unexplained until now, causes the near-UV SMF to degrade over time during operation with 405 nm lasers. In light of information obtained from users and manufacturers of fibre-coupled 405 nm diode laser systems, the time for an output power loss of 50 % or more to be reached varies from a few days to a few weeks. In this work, damage brought about on synthetic silica SMF by irradiation with high-power 405 nm diode lasers is reported. It is important to notice that the photon energy at this wavelength used in this work is much lower than the energy of the deep-UV absorption bands and the power density that is achieved is three orders of magnitude lower than the optical damage threshold.

## 2 EXPERIMENTAL SET-UP

For the irradiation of the fibre samples, two GaN diode laser modules offering high-power at 405 nm (Nichia) are used. The parameters listed in Table 1 for the multi-mode (MML) and single-mode lasers (SML) used in this work are achieved with the beam shaping optics in the modules. The SML is linearly polarised, while the MML consists of two linearly polarised diodes which are cross-combined. The modules are appropriately current and temperature stabilised to achieve a consistent output power. For the irradiation of the fibre, its proximal end was aligned to the maximum fibre output power using a very stable mechanical fibre alignment system. A thermopile power meter of type Coherent PowerMax PS19Q with a circular aperture of 19 mm was used to monitor the power received.

All fibres used have undoped synthetic silica cores and fluorine-doped claddings, with the low-mode fibre (LMF) having a core diameter of 10  $\mu\text{m}$  and the SMF having mode-field diameters in the range of  $2 \cdot w_0 = 2.5$  to  $3.2 \mu\text{m}$ . All the fibres used were stored for several months before irradiation. The fibres under test (FUT) had a length of 1 m, suitable for long-term experiments. For short-term experiments with the LMF discussed here, a length of 0.5 m was chosen due to the strong absorption in the deep-UV. Table 2 shows a matrix of the power density  $I_{core} = P_{out,fibre}/\pi \cdot w_0^2$  in the fibre core for various combinations of diode laser modules and fibre types. The actual power density experienced by the proximal fibre surface is in the range defined by  $I_{spots}$ , as given in Table 1.

The fibre output power can be stabilised at a level above 50 mW for several days by tracking the fibre input power. In this case a constant power density at the distal surface of  $I_{core} > 0.5 \text{ MW/cm}^2$  is achieved.

The end surfaces of the fibre samples were prepared by use of a standard cleaving technique and were cleaved shortly before being used in each experiment. The surface roughness was measured using atomic force microscopy (AFM) according to standardised techniques [15,16,17]. The average roughness for the cleaved samples was approximately 0.4 nm. During irradiation, the proximal fibre end is used inside the alignment system, but not sealed or flushed with gas. The distal end is in free space and not protected from dust particles. All experiments are conducted in a standard laboratory environment at room temperature.

The approach in this work has combined the use of light microscopy, which was undertaken immediately after irradiation, with further examination of the fibre end surfaces using both, atomic force microscopy (AFM) and scanning electron microscopy (SEM). In addition, under circumstances where samples were particularly interesting, energy dispersive x-ray (EDX) analysis was performed on particular samples. Further, for two particular samples, high resolution transmission electron microscopy (HR-TEM) was used for analysing a focused ion beam (FIB) prepared lamella.

The progress of the fibre damage during the irradiation period was monitored using the fibre output power from the fibre samples. The long-term experiments were undertaken over a period ranging from four days to two weeks, depending on the reduction in the fibre output power that was experienced. The goal for long-term damage was a power reduction in the range of 20 to 70 %, depending on the particular study being undertaken. The single short-term experiment with the LMF consisted of three exposure periods with a length of 5, 10, and 15 minutes, with spectral measurements being taken between exposures.

In order to determine spectrally induced loss, spectral measurements were taken before and after irradiation with light from the diode lasers. A recently developed spectrometer system, including a deuterium lamp as a broadband light source and a spectrometer with a back-thinned CCD chip measuring from 167 nm to 622 nm, was used to measure the SMF in the deep-UV. Short pieces of MMF with low solarisation were used for coupling in and out of the FUTs through butt-

coupling [6,7]. This procedure showed best reliability when repeatedly changing between the laser and the broadband system. In spite of that, some of the measurement samples show white light interference due to misalignment at the coupling sites. The dark current reading was subtracted from the recorded spectra and the result obtained was then processed using the relationship  $L_{ind}(\lambda) = -10 \log_{10}(I_{after}(\lambda) / I_{before}(\lambda))$  to monitor the spectral loss induced by 405 nm irradiation. This system was also used to determine the attenuation profile,  $\alpha(\lambda)$ , of the LMF by using the cut-back method. The fibre was thus cut back from 0.5 m to 0.25 m and the attenuation profile calculated by using the relationship  $\alpha(\lambda) = -10/l \cdot \log_{10}(I_{0.5m}(\lambda)/I_{0.25m}(\lambda))$  with  $l = 0.25$  m.

To determine the error in the power reading, the standard deviation of the daily average is added to the uncertainties seen from the power meter and the diode laser module. In the spectral measurements, a lamp signal error  $\Delta I$  of  $\pm 3$  % at 200 nm,  $\pm 2$  % at 300 nm and  $\pm 1$  % at 400 nm is taken into consideration. The noise in the spectrometer is much lower than this error and not taken into account. For the error of the spectral loss,  $\Delta L_{ind}$ , the non-linear propagation of error is used

$$\text{where } \Delta L_{ind} = \sqrt{(\partial L_{ind} / \partial I_{before})^2 \cdot \Delta I_{before}^2 + (\partial L_{ind} / \partial I_{after})^2 \cdot \Delta I_{after}^2}.$$

### 3 RESULTS

Figure 1 shows the output power for the two SMF samples presented here. Over the course of 9 days the reduction in fibre output power is 30 % for the sample irradiated with the MML. For the sample irradiated with the SML the output power reduced by 67 % within a period of 11 days. In both cases a stable long-term irradiation with the maximum fibre output power was achieved and a structural modification to the proximal fibre surface could be seen. Either a cross shape, if damaged with the MML, or a spot, if damaged with the SML, was observed by using light microscopy. With the use of AFM, a ripple structure on the protruding structure was discovered. Figure 2 shows the core region of the SMF sample damaged with MML for 9 days, the structure in this case had a height of about 500 nm. Figure 3 shows the core region of the SMF sample damaged with SML for 11 days, this structure had a height of about 700 nm. In both cases, the structure lies on the fibre core and spreads onto the cladding.

A ripple-like periodicity of 250 to 400 nm was determined for MML as well as for SML damage spots (see inset in Figure 3). The polarisation is denoted by the arrows in both figures and the ripples are oriented parallel to the polarisation direction of the laser light. In case of the MML damaged samples, the ripples run parallel the slow axes of the two laser spots along which the laser beams are polarised [18]. In the centre of the cross shape the ripples become very short and are more formed like cones.

The reduction in fibre output power is a strong indication not only of the clarity of the ripple, but also for the height of the structure. The surface structure grows out of the surface, protruding in some cases by more than 1  $\mu\text{m}$  with a base diameter of 3 to 6  $\mu\text{m}$ .

Figure 4 shows a REM image of a distal fibre end surface, that had been exposed to a constant power density  $I_{core} > 1 \text{ MW/cm}^2$  in the core for 8 days. This is also the power density on the distal end surface. A periodic structure was formed on the distal surface, but it does not cover the whole core and has a diameter of about 1  $\mu\text{m}$ . The structure is centred on the core at the point of highest intensity of the Gaussian light distribution, which is higher than the mean value  $I_{core}$ . The periodicity of the ripples is also about 250 to 300 nm as for the structure on the proximal surface. In addition, very small spherical and angular particles aggregate in a radius of about 5  $\mu\text{m}$  around the centre of the fibre. These particles were not seen on the freshly cleaved surface, which was observed to be ‘perfectly’ clean.

EDX analyses on several different samples from the proximal and distal end have repeatedly shown no variation in the elemental concentrations between the core and its structure, and the area around it. The aggregated particles found on the distal end also showed no trace of this in the EDX analyses. A high resolution transmission electron microscope (HR-TEM) image of a 150 nm thick focused ion beam (FIB) prepared lamella of a MML damage spot is presented in Figure 5. It shows that the damaged area is a layer with lower material density (area *b* in lighter grey). Below this surface layer and outside of the irradiated area the material density is unchanged (area *c* in darker grey). The surface region of the lower density material has a porous structure. No diffraction patterns indicating crystalline structures were seen in the TEM.

The calculated loss spectra  $L_{ind}(\lambda)$  of the short-term irradiated LMF sample showed no degradation at 405 nm. On the other hand, a change in fibre attenuation in the deep-UV could be observed in Figure 6. The spectral loss at 245 nm, seen as an absorption peak in the attenuation profile in the inset of Figure 6, reduces within minutes, while loss below 240 nm is increased. The LMF sample shows some white light interference effects in the wavelength range of 270 to 400 nm, due to slightly different coupling conditions before and after irradiation. The effect of the white light interference is not included in the error. The induced loss below 240 nm increases with the total irradiation time and likely masks the increase of the induced gain at 250 nm. The induced loss values, at wavelengths below 220 nm could not readily be calculated, because of the increasing strong absorption and limited dynamic of the measurement system.

The induced loss was also observed for SMF samples, when they were irradiated for a few days only. In this case the reduction of the fibre output power was below 20 %. The change in fibre attenuation of the SMF sample in Figure 7 is not as strong as for the LMF sample, but peaks at wavelengths of 215 and 250 nm are clearly visible. However, when the SMF is irradiated for extended periods a broadband loss is observed from the red down into the deep-UV. The loss decreases with the use of longer wavelengths.

## 4 DISCUSSION

The change of the fibre absorption in the deep-UV occurs at the oxygen deficient centre ODC(II) at 245 nm and the  $E'_\gamma$  centre at 214 nm [10,11]. The ODC(II) is an unrelaxed oxygen vacancy or a divalent silicon bond, which in our case are precursors for defect centres [5]. A transformation of the ODC(II) centres (5 eV) into  $E'_\gamma$  centres (5.8 eV), with an unpaired  $sp^3$  electron, can be explained in several ways. A transformation through coherent two-photon absorption of 405 nm (3 eV) photons seems unlikely in a low power experiment of this type, but the probability of this increases with the extremely long exposure. A two-step process is also possible [19] – if an exciton is generated when two consecutive photons are absorbed incoherently, then a non-radiative decay of the exciton can induce an  $E'_\gamma$  centre close to the absorption site. On the other hand,  $E'_\gamma$  centres can be generated directly at the absorption site by a two-step ionisation of ODC(II) centres.

Nevertheless, this transformation reduces the number of ODC(II) centres and increases the number of  $E'_\gamma$  centres. As reported in the introduction, this bleaching of ODC(II) is also known from excimer laser experiments [13]. Since the fibres were stored for a long time before irradiation, all molecular  $H_2$  remaining from their production should be reduced to atmospheric concentrations within the 125  $\mu\text{m}$  fibres. In this case a passivation of defects from molecular  $H_2$  is neglectable. The immediate reduction of the ODC(II), compared to the increase of  $E'_\gamma$  centres over time, points towards a two-step process generating excitons which decay, over time, inducing the  $E'_\gamma$  centres. These deep-UV effects of 405 nm laser irradiation need further investigation to reveal the actual mechanism involved.

The absorption change can only be seen in the LMF samples and short-term irradiated SMF samples. The damaged area of 6  $\mu\text{m}$  in diameter on the 15  $\mu\text{m}$  core LMF is over-illuminated by the deuterium lamp. Thus the damage spot at the proximal surface cannot interfere with the loss measurement. If the surface structure is very distinct and covers the whole core, e.g. of the SMF, then the structure interferes with the light coupling into the fibre and only the mentioned broadband loss can be observed. This broadband power loss is the result of focusing and scattering by the periodic surface structure on the proximal fibre end, impairing the coupling efficiency. The structure on the distal end would not be expected to reduce the power transmitted by the fibre, but would impair the quality of the beam radiated from the fibre end surface. An investigation of these effects on transmission and on the beam quality in more detail is part of on-going work.

In the experiments carried out at a wavelength of 405 nm, the CW power density  $I_{spot}$  in the laser beam waist and  $I_{core}$  in the fibre core and on the distal fibre surface was at least in the range of 0.5 to 1 MW/cm<sup>2</sup>. Maximum values of 2.5 MW/cm<sup>2</sup> are obtained when the laser and fibre are operating in the single-mode regime. This is still three orders of magnitude lower than the optical damage threshold of more than 1 GW/cm<sup>2</sup>. Nevertheless, a deformation of the synthetic silica surface over a duration of several days is observed.

Similar periodic surface structures with ripples, called laser induced periodic surface structures (LIPSS), were seen in short-pulsed laser experiments on mostly crystalline wide band-gap materials [20,21,22]. Those structures also exhibit bifurcations, bends and break-ups, as is seen in the case here. The current model explains these structures by self-organisation of an unstable surface layer by duelling processes of desorption and self-diffusion [23]. In the past, an interference model was used to describe these effects, but in the last decades new results and simulations have been presented to contradict this model [24,25,26].

It is suggested in this work that the fibre surface is destabilised by a multi-step surface ionisation leading to Coulomb explosion, i.e. desorption. The surface ionisation starts with the generation of unpaired electrons on or close to the surface through two-photon absorption. The  $E'_\gamma$  centres are generated either from ODC(II) as in the bulk of the fibre or from silanone and dioxasilirane surface centres [5]. The unpaired electrons can be excited further and above a certain threshold escape from the surface leaving a positively charged surface behind.

If the fibre output power is high enough over a period of several days, then the same effects are seen on the distal fibre surface. The aggregation of very small particles on the core region of the distal fibre surface is also an indication for a surface ionisation. Either charged atomic clusters are repelled out of the surface or external particles are attracted to the charged surface.

The periodic surface structure on the distal fibre surface also shows that the formation of the periodic structures depends on the power density. It only appears in the region of highest intensity of the Gaussian light distribution in the core. On the proximal fibre surface, where the power density is higher overall, the structure appears on the whole core.

The laser and material parameters contributing to the generation of periodic surface structures with short-pulsed laser experiments correspond to the important parameters that were found [23,27,28]. The thickness of the unstable layer is seen to increase with power density, surface roughness and the generation of defect centres. The form and orientation of the ripples depend strongly on the laser polarisation. In the work reported here on silica fibres, the structural orientation of the ripples correlates with the polarisation direction of the laser light. In case of the cross-polarised laser light short ripples and cones are observed, just as for elliptical and circular polarised light in the work of Varlamova et.al.[29].

The formation of the periodic surface structure is a modification of the silica on the surface. It was found that there was no difference in the chemical composition between the core region and the region around it in the EDX analyses. The TEM images showed that there is a surface layer in the area of irradiation with a lower density than the silica material around it. This layer of lower density has a porous structure in its outermost part. Since no diffraction patterns were observed in the TEM, it can be concluded that it is not crystalline but is rather an amorphous layer of lower density silica.

In this research, the fibre end surfaces were not explicitly protected from the environment. Thus, dust particles attracted by an ionised surface and water absorbed by the silica should not be ruled out as triggers of the modification effects seen.

However, no other elements beside silicon, oxygen and the sputter specimen were found in significant quantities in the fibre core area by EDX analyses, carried out so far. Additionally, the heating of absorbed water in the fibre core is not likely at the short wavelength of 405 nm used. The need for further investigation of this is recognized and long-term experiments with fibre end surfaces in a box flushed with different inert gases are a key part of on-going research.

## 5 CONCLUSION

It has been shown that the damage occurring on proximal and distal silica fibre surfaces during irradiation is due to the generation of a periodic surface structure, impairing the coupling efficiency and the beam quality. It is suggested in this work that this ripple structure is formed by a self-organising process of an unstable surface layer of silica. The generation of  $E'_\gamma$  centres enhances the surface ionisation and thus the destabilisation.

## 6 ACKNOWLEDGEMENTS

The authors would like to acknowledge support from the German Federal Ministry of Education and Research through AiF under grant FKZ 1737X08. In addition we would like to thank Jan Heimann for discussion and his contribution to the experimental work, Elke Landrock-Bill for the SEM and EDX analyses, Omicron-Laserage GmbH for providing the UV diode lasers, Prof. Georg Hillrichs from the University of Applied Sciences Merseburg and the Fraunhofer Institute for Mechanics of Materials in Halle for the AFM and HR-TEM analyses. Support from the UK Engineering & Physical Sciences Research Council (EPSRC) for the UK team is gratefully acknowledged.

## REFERENCES

- [1] D.L. Griscom, *J. Non-Cryst. Solids* 73 (1985) 51-78.
- [2] E.J. Friebele, D.L. Griscom, in: M. Tomozawa, R.H. Doremus (Eds.), *Treatise on materials science and technology: Glass II*, Academic Press St. Louis, 1979, pp. 257-351.
- [3] E.J. Friebele, G.H. Sigel, D.L. Griscom, *Applied Physics Letters* 28(1976) 516-518.
- [4] V.K. Khalilov, G.A. Dorfman, E.B. Danilov, M.I. Guskov, V.E. Ermakov, *J. Non-Cryst. Solids* 169 (1994) 15-28.
- [5] L. Skuja, *J. Non-Cryst. Solids* 239 (1998) 16-48.
- [6] K.-F. Klein, R. Arndt, G. Hillrichs, M. Ruetting, M. Veidemanis, R. Dreiskemper, J.P. Clarkin, G.W. Nelson, *Proc. SPIE* 4253 (2001) 42.
- [7] V.K. Khalilov, K.-F. Klein, J. Belmahdi, R. Timmerman, G.W. Nelson, *Proc. SPIE* 6083 (2006) 08.

- [8] M. Dressel, R. Jahn, W. Neu, K. Jungbluth, *Laser. Surg. Med.* 11 (1991) 569-579.
- [9] M. Koehler, H. Dietz, Y. Matsuura, M. Miyagi, K.F. Klein, G. Hillrichs, *Proc. SPIE* 4957 (2003) 92-96.
- [10] R. Pini, R. Salimbeni, M. Vannini, *Appl. Opt.* 26 (1987) 4185-4189.
- [11] K.-F. Klein, G. Hillrichs, P. Karlitschek, K. Mann, *Proc. SPIE* 2966(1996) 564-573.
- [12] H. Imai, K. Arai, H. Imagawa, H. Hosono, Y. Abe, *Phys. Rev. B* 38 (1988) 12772-12775.
- [13] H. Imai, K. Arai, H. Hosono, Y. Abe, T. Arai, H. Imagawa, *Phys. Rev. B* 44 (1991) 4812-4818.
- [14] M.R. Kirshenbaum, E.J. Seibel, *Proc. SPIE* 7894 (2011) 13.
- [15] DIN EN ISO 4287:2010, Geometrical Product Specifications (GPS) - Surface texture: Profile method - Terms, definitions and surface texture parameters
- [16] DIN EN ISO 4288:1998, Geometrical Product Specifications (GPS) - Surface texture: Profile method - Rules and procedures for the assessment of surface texture
- [17] DIN EN ISO 3274:1998, Geometrical Product Specifications (GPS) - Surface texture: Profile method - Nominal characteristics of contact (stylus) instruments
- [18] M. Mansuripur, E.M. Wright, *Opt. Photonics News* 13(2002) 57-61.
- [19] F. Messina, M. Cannas, R. Boscaino, *J. Phys.: Condens. Matter* 20 (2008) 275210.
- [20] M. Birnbaum, *J. Appl. Phys.* 36 (1965) 3688.
- [21] F. Keilmann, Y.H. Bai, *Appl. Phys. A: Mater.* 29 (1982) 9-18.
- [22] H.M. van Driel, J.E. Sipe, J.F. Young, *Phys. Rev. Lett.* 49 (1982) 1955-1958.
- [23] J. Reif, F.A. Costache, M. Bestehorn, in: J. Perrière, E. Millon, E. Fogarassy (Eds.), *Recent advances in laser processing of materials*, Elsevier Ltd. Kidlington, 2006, pp. 275-290.
- [24] J.S. Preston, H.M. van Driel, J.E. Sipe, *Phys. Rev. B* 40(1989) 3942-3954.
- [25] J. Reif, F.A. Costache, S. Eckert, S. Kouteva-Arguirova, M. Bestehorn, I. Georgescu, A.F. Semerok, P. Martin, O. Gobert, W. Seifert, *Proc. SPIE* 5662 (2004) 737.
- [26] J. Reif, O. Varlamova, M. Bounhalli, T. Arguirov, M. Schade, H.S. Leipner, *Proc. SPIE* 7586 (2010) 0H.
- [27] M. Henyk, N. Vogel, D. Wolframm, A. Tempel, J. Reif, *Appl. Phys. A: Mater.* 69 (1999) S355-S358.
- [28] J. Reif, *Opt. Eng.* 28 (1989) 1122-1132.
- [29] O. Varlamova, F.A. Costache, M. Ratzke, J. Reif, *Appl. Surf. Sci.* 253 (2007) 7932-7936.

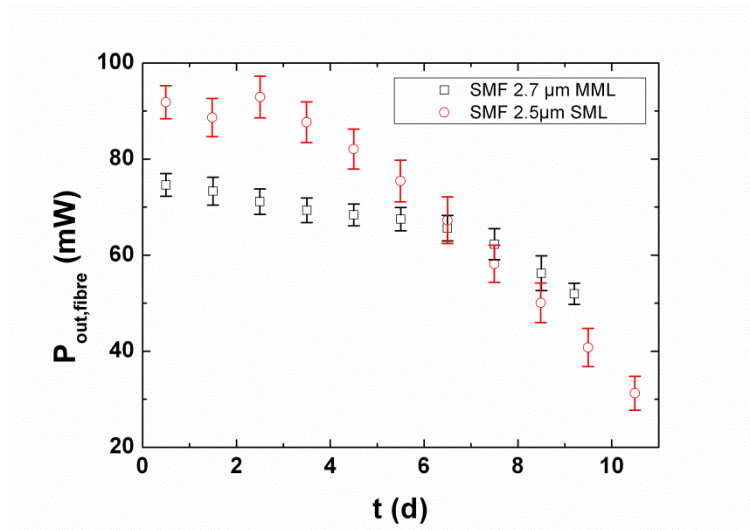


Figure 1: Fibre output power  $P_{out,fibre}$  over time of two 1 m long SMF samples irradiated with either MML or SML. Each data point represents the daily average of output power.

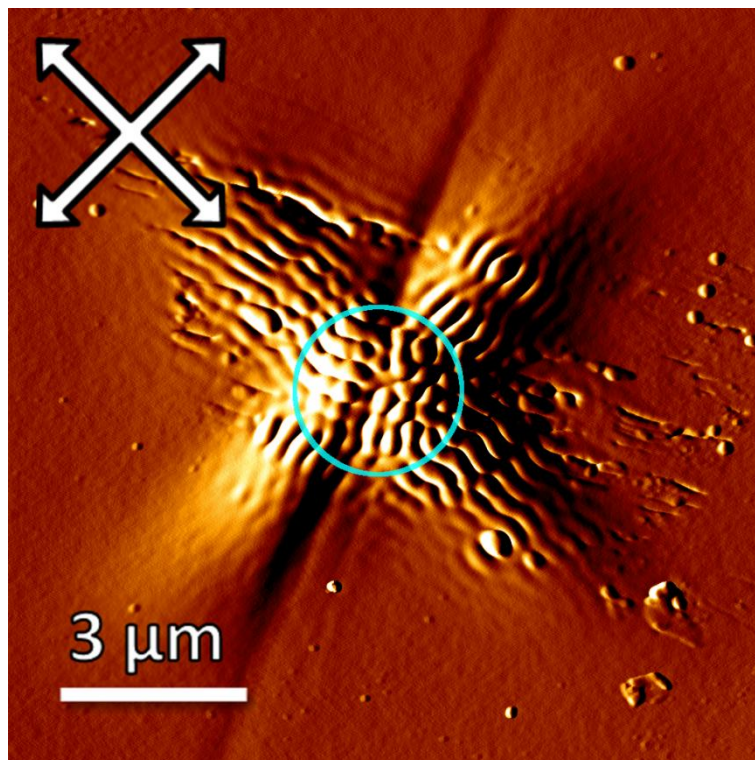


Figure 2: AFM micrograph of the proximal end of a cleaved SMF damaged with MML for 9 days. The size of the mode-field diameter of the fibre is denoted by a circle. The depressed line going through the cross shape is erosion from an EDX line scan.

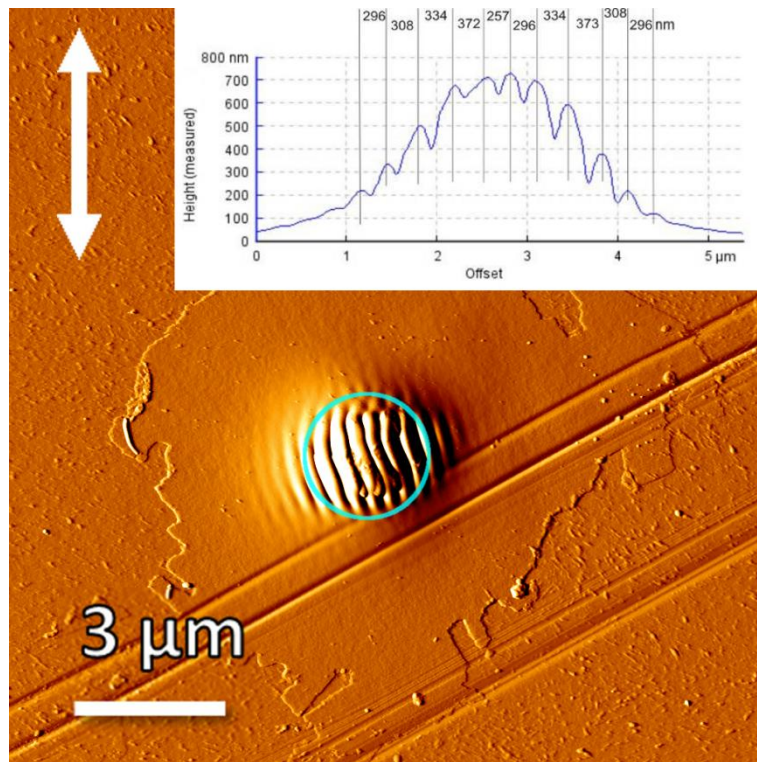


Figure 3: AFM micrograph of the proximal end of a cleaved SMF damaged with SML for 11 days. The size of the mode-field diameter of the fibre is denoted by a circle. The scratches running across the surface are from the cleaving process. The inset shows a height line scan across the periodic structure.

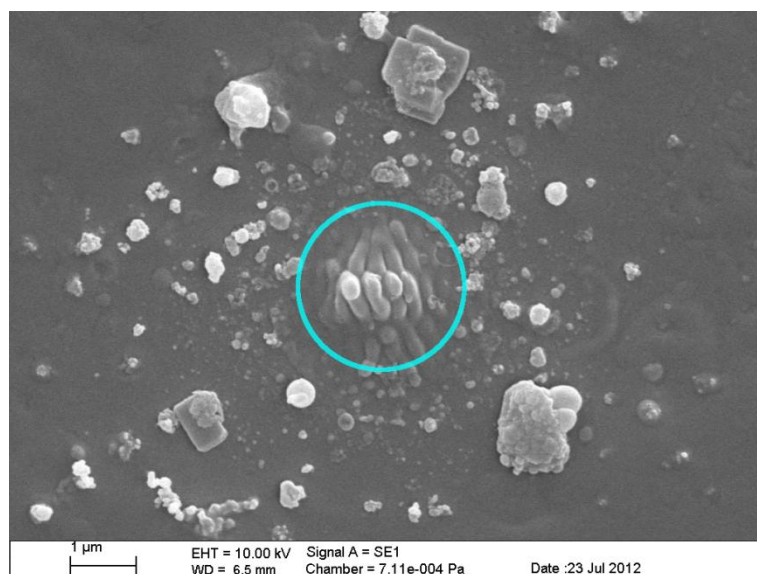


Figure 4: SEM image of the distal end of a cleaved SMF damaged with constant power density  $I_{core} > 1 \text{ MW/cm}^2$  for 8 days. The size of the mode-field diameter of the fibre is denoted by a circle.

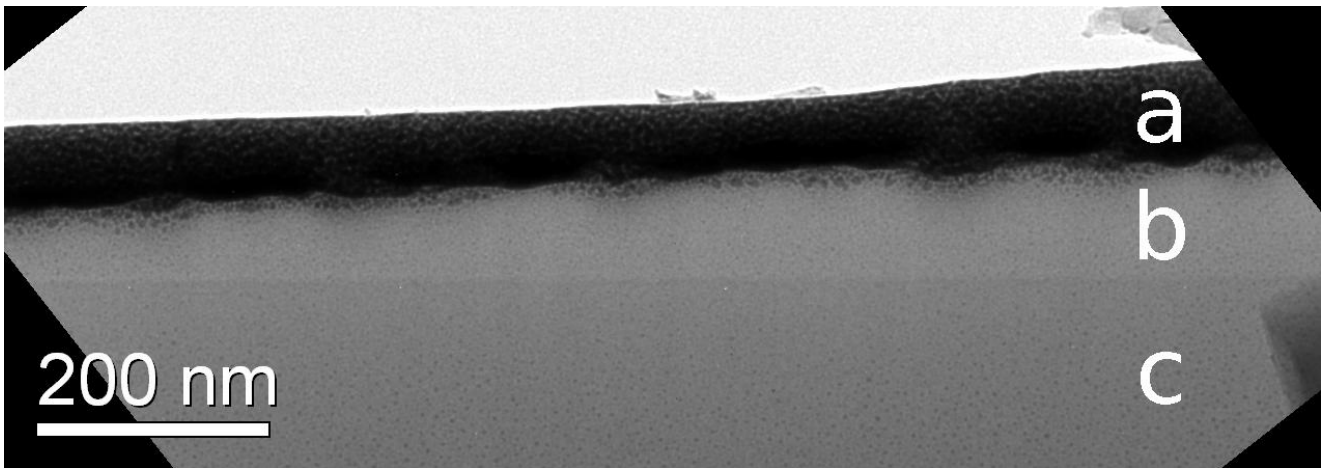


Figure 5: HR-TEM image of a FIB lamella of a MML damage spot. On top is the sputter specimen platinum (*a*, black), below a porous, lower density silica material (*b*, lighter grey), and further below unchanged fibre material (*c*, darker grey).

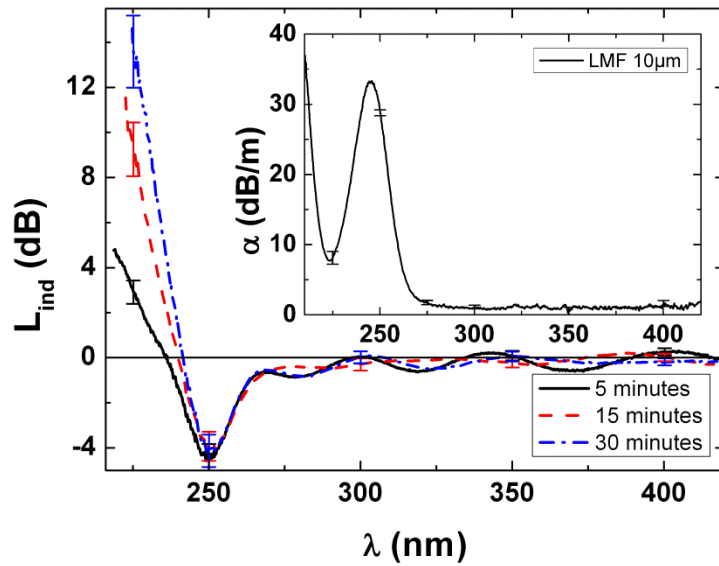


Figure 6: Loss spectra  $L_{ind}(\lambda)$  of a 0.5 m LMF sample with a core diameter of 10  $\mu\text{m}$  and a length of 0.5 m for the given irradiation times with the MML. This sample exhibits some effects due to white light interference. The inset shows the attenuation profile of this fibre type.

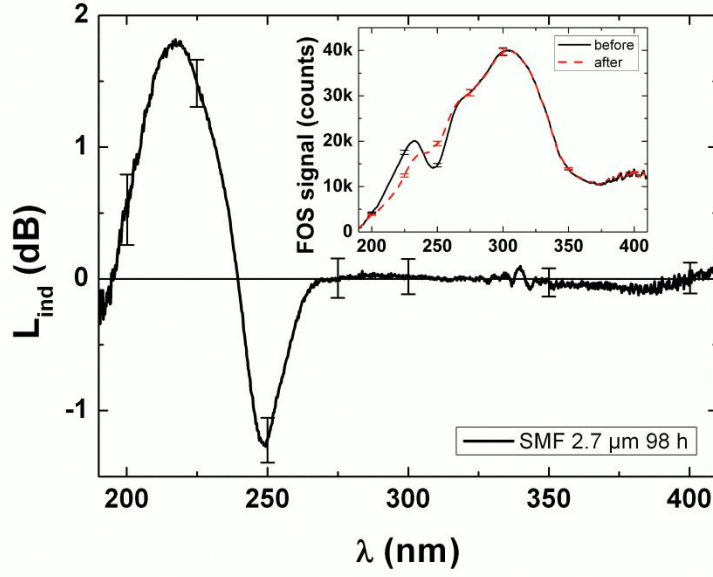


Figure 7: Loss spectrum  $L_{ind}(\lambda)$  of a SMF sample with a mode-field diameter of  $2.7 \mu\text{m}$  and a length of  $1 \text{ m}$  for an irradiation time of  $98 \text{ h}$  with the MML. The inset shows the fibre-optic spectrometer (FOS) spectra taken before and after irradiation.

Parameter	MML double diode	SML
Number of laser diodes	2 (cross-polarised)	1
Output power $P_{out} / \text{mW}$	$300 \pm 5$	$150 \pm 3$
Power stability $\Delta P_{out} / \% / \text{h}$	$< 0.25$	$< 0.4$
Calculated spot diameter $2 \cdot w_0 / \mu\text{m}$	5.9	2.78
Calculated power density in spot $I_{spot} / \text{MW}/\text{cm}^2$	1.1	2.45

Table 1: Summary of characteristics of the diode laser modules used.

	MML	SML
<b>LMF</b>	$I_{core} = 100 - 130 \text{ kW}/\text{cm}^2$	N/A
<b>SMF</b>	$I_{core} = 0.9 - 1.3 \text{ MW}/\text{cm}^2$	$I_{core} = 1.6 - 2 \text{ MW}/\text{cm}^2$

Table 2: Data for the power density  $I_{core}$  in the fibre core for various combinations of diode laser modules and fibre types.